



Strål
säkerhets
myndigheten

Swedish Radiation Safety Authority

Author: Daniel Mångård

Research

2017:16

Stress intensity factor solutions for circumferential cracks in cylindrical bars under axisymmetric loading and global bending

SSM perspective

Background

The case of a circumferential crack in a cylindrical bar has not been available in the ProSACC code. The need for such a geometry, especially considering nonlinear axisymmetric loading and global bending, has motivated the development of new stress intensity factor solutions, also known as *K*-solutions. These new *K*-solutions will be available in ISAAC, the successor to ProSACC.

Objectives

The objective is to implement a capability in the computer code ISAAC to analyze long circumferential cracks in solid bars that may occur, for example due to thermal fatigue loadings. This means that both nonlinear axisymmetric loading and global bending loads have to be taken into account.

Results

The *K*-solutions, which have been numerically determined, account for axisymmetric loading up to the 5th degree as well as global bending. The new *K*-solutions are limited by the crack depth $a/R \leq 0.8$ which is a limit applied in ISAAC.

Verification of the new *K*-solutions has been performed against available reference solutions and numerical results specifically obtained for selected cases.

A degree of conservatism is introduced in the *K*-solutions as nonlinearities due to contact between crack faces from global bending loads have been omitted. The degree of conservatism is discussed in appendix A.

Project information

Contact person SSM: Daniel Kjellin

Reference: SSM2016-614



Strål
säkerhets
myndigheten

Swedish Radiation Safety Authority

Author: Daniel Mångård
Inspecta Technology AB, Stockholm

2017:16

Stress intensity factor solutions for circumferential cracks in cylindrical bars under axisymmetric loading and global bending

Date: March 2017

Report number: 2017:16 ISSN: 2000-0456

Available at www.stralsakerhetsmyndigheten.se

This report concerns a study which has been conducted for the Swedish Radiation Safety Authority, SSM. The conclusions and viewpoints presented in the report are those of the author/authors and do not necessarily coincide with those of the SSM.

Contents

1. Introduction	2
2. Problem statement	2
2.1 Existing <i>K</i> -solutions.....	2
2.2 New <i>K</i> -solutions.....	3
3. Method	4
4. Results	6
4.1 New geometry factors	6
4.2 Verification.....	8
5 References	10
A. Global bending and contact between the crack faces	11

1. Introduction

The case of a circumferential crack in a cylindrical bar is not available in ProSACC [1]. The need for such a geometry, especially considering nonlinear axisymmetric loading and global bending, has motivated the development of new stress intensity factor solutions, also known as K -solutions. The new K -solutions will be available in ISACC [2], the successor to ProSACC.

2. Problem statement

2.1 Existing K -solutions

K -solutions for a circumferential crack in a cylindrical bar subject to membrane tensile loading are available in e.g. [3] and [4]. Reference [4] also provides a solution for global bending. The accuracy of these solutions, expressed in terms of error, is stated to be less than 0.1 % in [3] and better than 1 % in [4].

The solutions are either expressed in or can be recast into the form of equation (1) where σ is the stress contribution, a is the crack depth and F is a non-dimensional stress intensity factor also referred to as a geometry factor. The geometry factor may be expressed as a function of the crack depth a and the bar radius R . The geometry is illustrated in Figure 1 where the crack depth is bounded by $0.0 \leq a/R \leq 1.0$.

$$K_I = \sigma\sqrt{\pi a} \cdot F(a/R) \quad (1)$$

The solutions in [3] and [4] are commonly referenced in the literature, handbooks, guidelines, and standards. However, there have been observations revealing an inconsistent reproduction of the solutions provided in [4], which are given in terms of net stress and uses the radius as a geometrical parameter. The inconsistencies appear e.g. by mistaking the net stress for nominal stress.

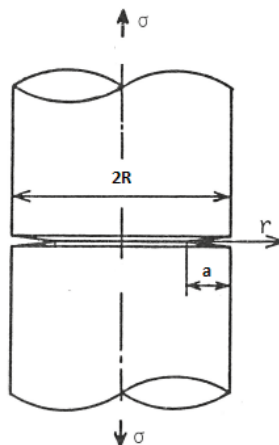


Figure 1 A circumferential crack in a cylindrical bar under tension [3].

2.2 New K -solutions

The K -solutions developed here cover axisymmetric loading up to the 5th degree as well as global bending, see equation (2) and (3) where the case $i = 0$ corresponds to membrane tensile loading. Geometry and loads are illustrated in Figure 2 and Figure 3.

The new K -solutions are limited by the crack depth $a/R \leq 0.8$ which is a limit that is commonly applied in ProSACC and ISAAC.

$$K_I = \sqrt{\pi a} \left(\sum_{i=0}^5 \sigma_i f_i + \sigma_{gb} f_{gb} \right) \quad (2)$$

$$\sigma = \sigma(r, z) = \sigma_{gb} \cdot \left(\frac{z}{R} \right) + \sum_{i=0}^5 \sigma_i \left(\frac{r}{R} \right)^i \quad (3)$$

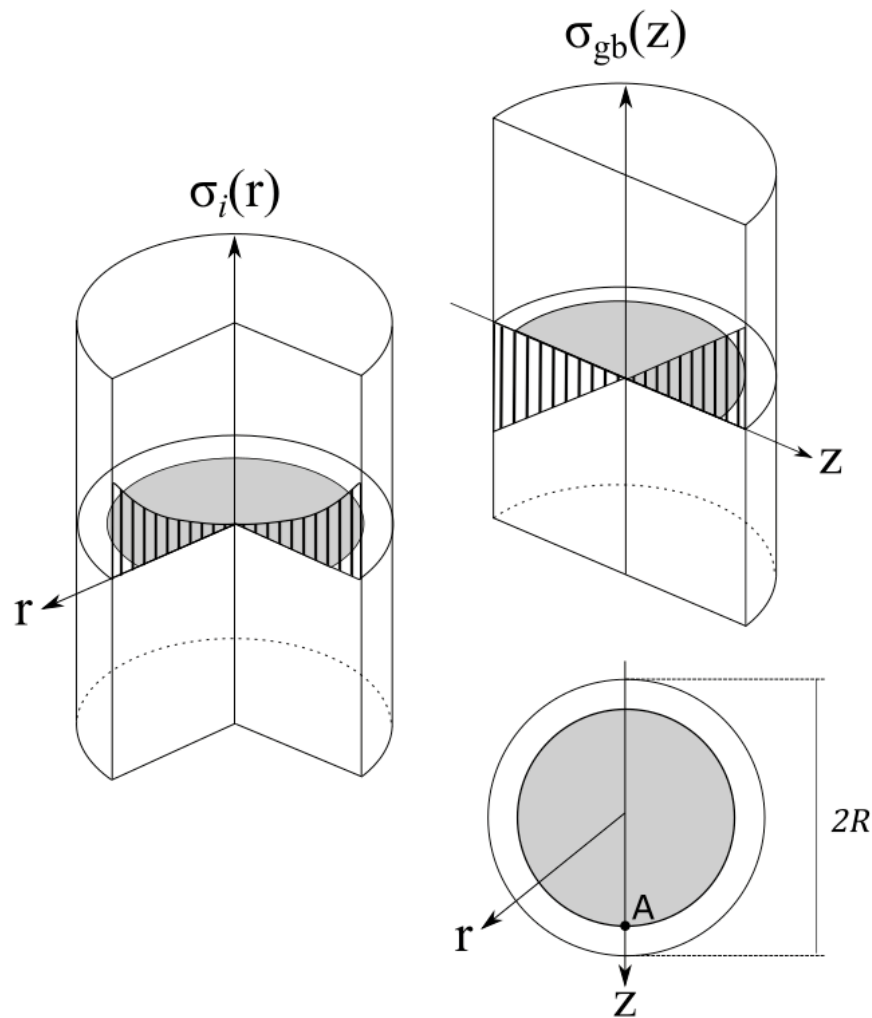


Figure 2 Illustration of a circumferential crack in a cylindrical bar under axisymmetric loading and global bending.

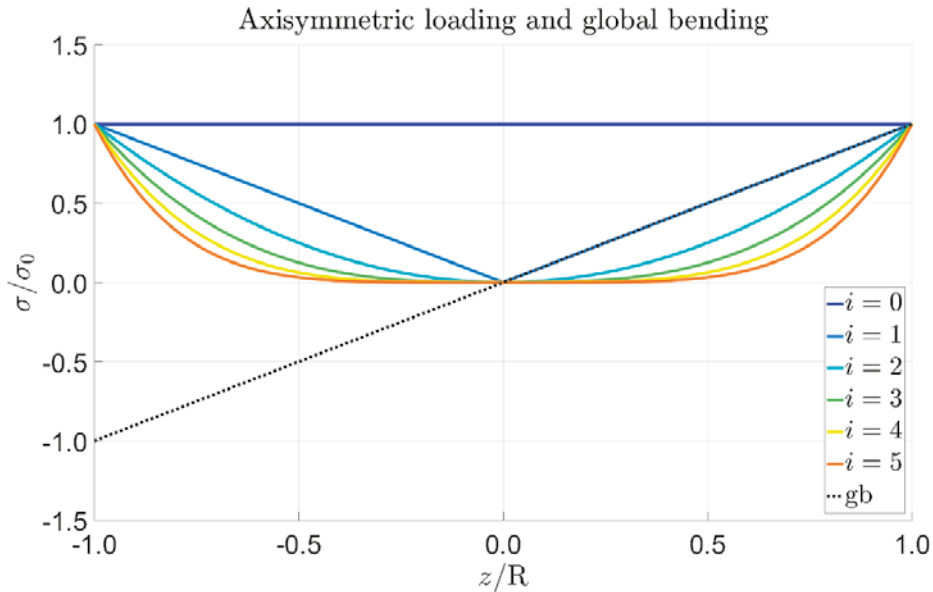


Figure 3 Axisymmetric loading and global bending.

3. Method

K -factors have been determined from 3D-FEM analyses performed with Abaqus [5]. The material has been assigned linear elastic material properties with $\nu = 0.3$.

Symmetry has been exploited in order to reduce the size of the models which all have the length $L = 20R$. The representative model for $a/R = 0.5$ corresponds to a quarter of the actual bar, see Figure 4.

The loading has been introduced as crack face pressure according to the principle of superposition. Axisymmetric loading results in either tensile or compressive stress across the entire crack face whereas global bending results in tensile as well as compressive stresses.

Eight equally spaced crack depths within the interval $0.0 \leq a/R \leq 0.8$ have been analyzed by 3D-FEM. Contact has not been included when the new K -factors have been determined.

The numerically computed K -factors are path independent and have been extracted at the crack front location corresponding to $z = R - a$, i.e. point A in Figure 2. The K -factor is constant along the circumference for axisymmetric loads, in contrast to global bending for which it varies along the circumference with the highest and lowest values observed at $z = R - a$ and $z = -R + a$, respectively.

Global bending may in reality give rise to contact between the crack faces. Omitting this contact in the analyses adds conservatism to the solution. A comparison of simulations with and without contact is given in Appendix A where it is shown that the conservatism increases with increasing crack depth.

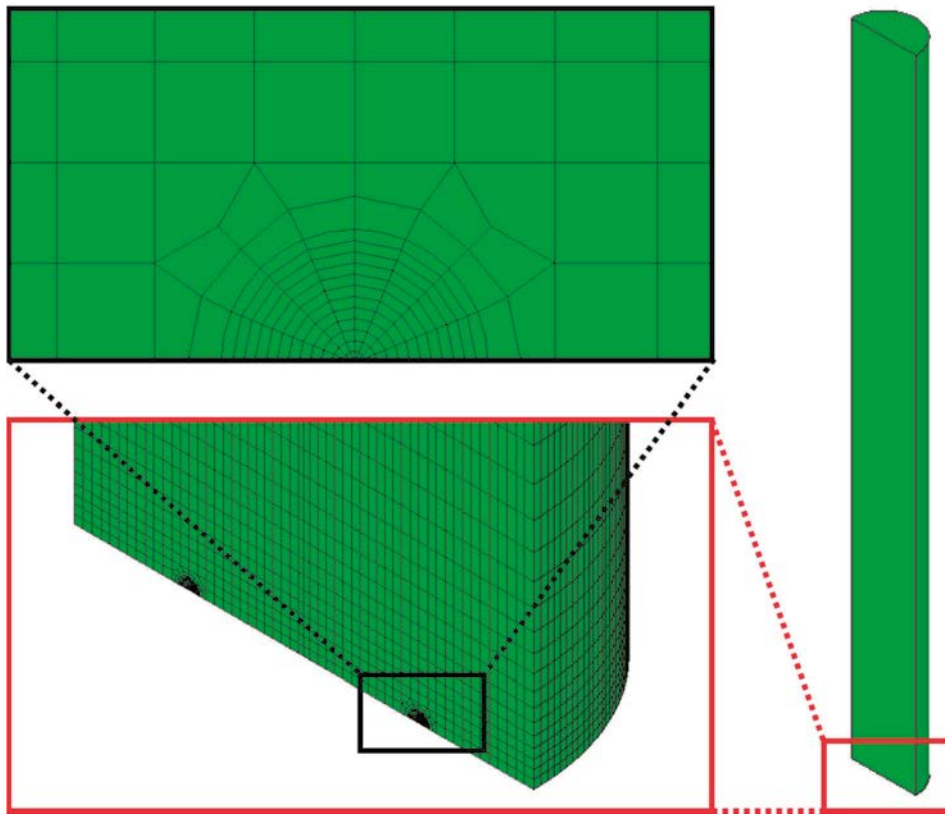


Figure 4 *FE-modelling for the crack depth $\alpha/R = 0.5$.*

4. Results

4.1 New geometry factors

Numerically determined geometry factors for axisymmetric loading and global bending are shown in Figure 5 and Figure 6, respectively. Table 1 shows tabulated geometry factors.

The numerical results for membrane tensile loading ($i = 0$) are in excellent agreement with the solution available in [3]. Excellent agreement is also observed for global bending in comparison with the solution available in [4]. For sufficiently small cracks ($a/R \rightarrow 0$), all axisymmetric loadings may be approximated as a membrane tensile load ($i = 0$). This implies that all geometry factors for axisymmetric loading converge towards the same value at $a/R = 0$.

For axisymmetric loading at $a/R = 0$, the solution available in [3] has been selected rather than determining a value by extrapolation of numerical results for larger crack depths. The same applies to global bending at $a/R = 0$ for the solution available in [4].

Table 1 *Geometry factors.*

a/R	f_{gb}	f_0	f_1	f_2	f_3	f_4	f_5
0.0	1.1242	1.1215	1.1215	1.1215	1.1215	1.1215	1.1215
0.1	1.1665	1.1808	1.1104	1.0452	0.9850	0.9294	0.8778
0.2	1.3161	1.2619	1.1147	0.9897	0.8832	0.7922	0.7142
0.3	1.5968	1.3927	1.1568	0.9734	0.8295	0.7156	0.6246
0.4	2.0876	1.6014	1.2550	1.0090	0.8308	0.6992	0.5999
0.5	2.9793	1.9385	1.4420	1.1199	0.9029	0.7512	0.6411
0.6	4.7728	2.5139	1.7904	1.3597	1.0861	0.9014	0.7698
0.7	9.0842	3.6150	2.4913	1.8712	1.4923	1.2403	1.0614
0.8	23.421	6.2377	4.2087	3.1520	2.5175	2.0961	1.7959

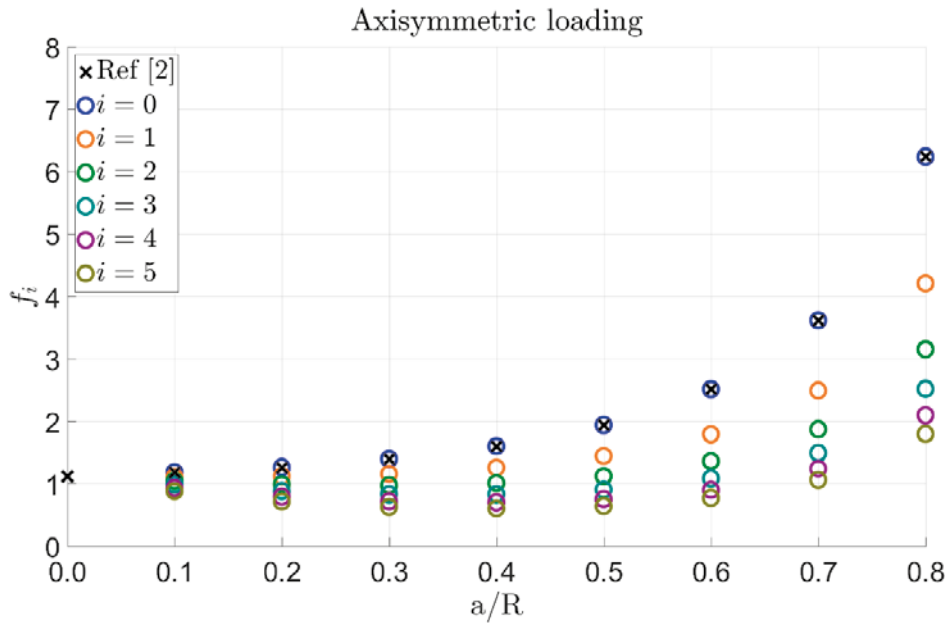


Figure 5 Geometry factors for axisymmetric loading.

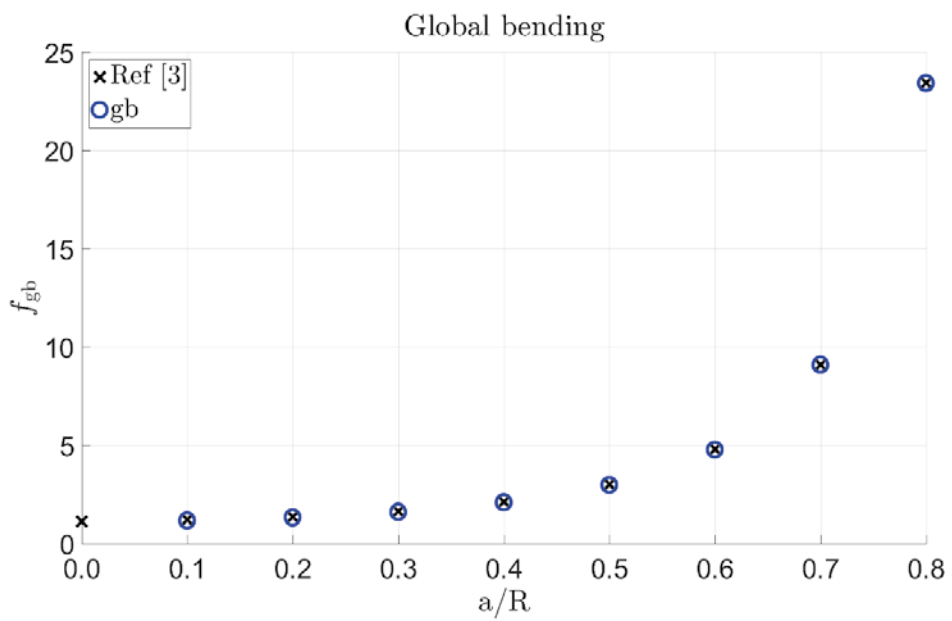


Figure 6 Geometry factors for global bending.

4.2 Verification

Verification of the new geometry factors has been performed against numerical results obtained for three different cases.

Case 1 corresponds to membrane tensile loading ($i = 0$) and is a further presentation of the results shown in Figure 5. Comparison of the new geometry factors and the solution in [3] shows an excellent agreement. Relative error in percent is shown in Figure 7 where K_{SOL} represents the new geometry factors developed in this work and K_{REF} represents the solution in [3].

Case 2 consists of both axisymmetric loading and global bending where the stress components have been arbitrarily chosen. The relative error in percent is shown in Figure 8 where K_{SOL} represents the solution using the new geometry factors developed in this work and K_{FEM} represents the numerical results (with contact omitted) for the specific loading.

$$\text{Case 2: } \begin{bmatrix} \sigma_{\text{gb}} \\ \sigma_0 \\ \sigma_1 \\ \sigma_2 \\ \sigma_3 \\ \sigma_4 \\ \sigma_5 \end{bmatrix} = \begin{bmatrix} 0.5581 \\ 0.4301 \\ 0.8074 \\ 0.7818 \\ -0.3317 \\ 0.3975 \\ -0.6044 \end{bmatrix}$$

Case 3 consists of an axisymmetric stress profile extracted from a cyclic thermal loading. The stress profile is shown in Figure 9. The relative error in percent is shown in Figure 10 where K_{SOL} represents the solution using the new geometry factors developed in this work and K_{FEM} represents the numerical results for the specific loading.

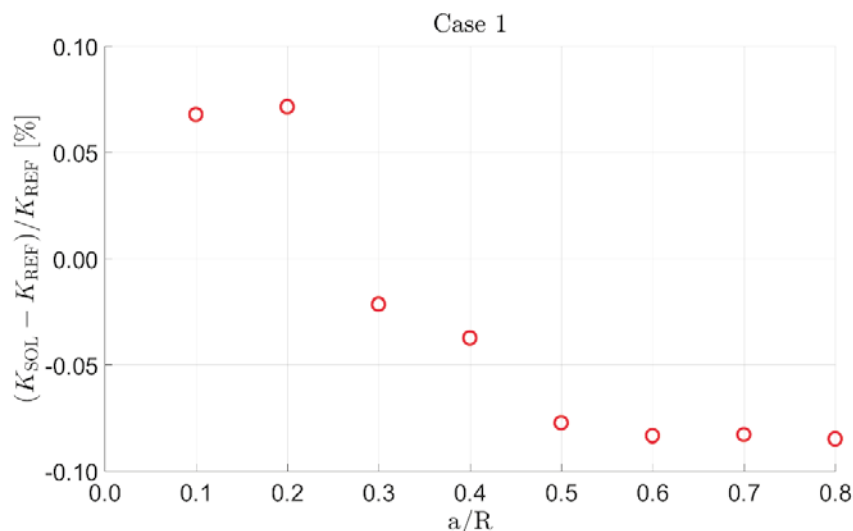


Figure 7 Relative error in percent for Case 1.

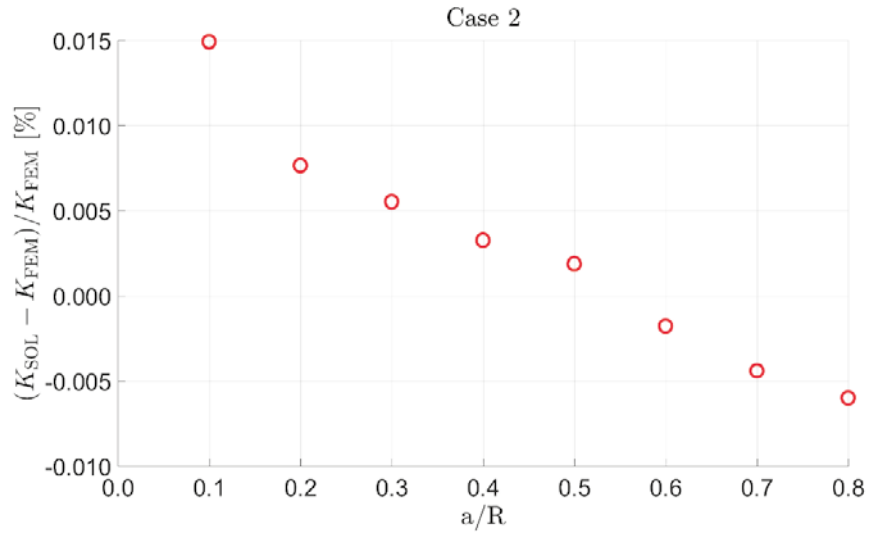


Figure 8 Relative error in percent for Case 2.

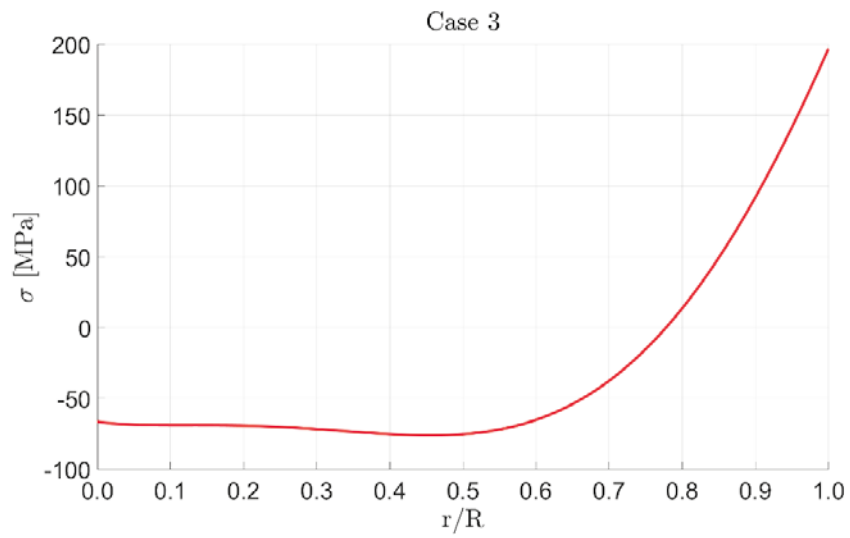


Figure 9 Axisymmetric loading for Case 3.

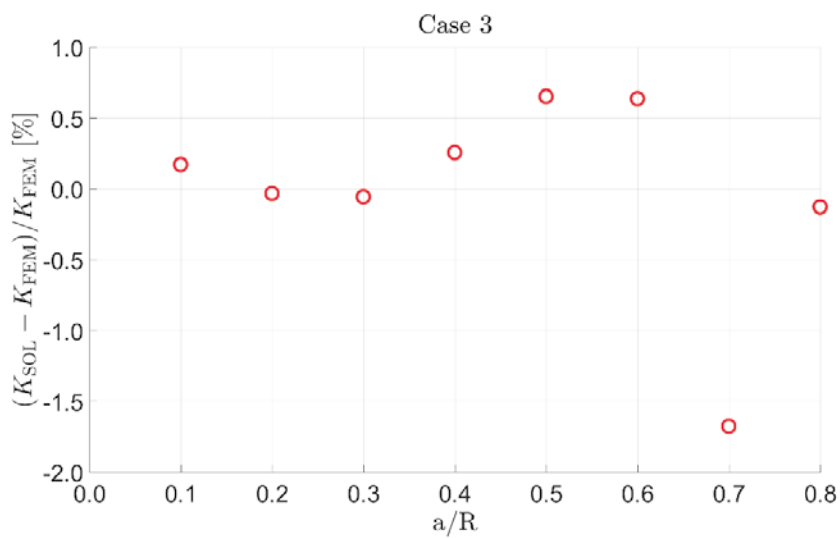


Figure 10 Relative error in percent for Case 3.

5 References

- [1] Dillström P, Bergman M, Brickstad B, et al., "A combined deterministic and probabilistic procedure for safety assessment of components with cracks - Handbook," Strålsäkerhetsmyndigheten, 2008.
- [2] "Procedure for Safety Assessment of Components With Defects – Handbook Edition 5," Technical Report No 2017-50010860-1, Inspecta Technology AB, 2017 (to be published by SSM).
- [3] Y. Murakami, Ed., Stress Intensity Factors Handbook, 1987.
- [4] Tada, H., Paris, P. & Irwin, G., "The stress analysis of cracks handbook," MA: Del Research Corporation, Hellertown, 1973.
- [5] Dassault Systemes, *ABAQUS version 6.14*.

A. Global bending and contact between the crack faces

Contact has not been included when the new K-factors have been determined. Omitting this contact in the analyses adds conservatism to the solution. In reality, however, global bending may give rise to contact between the crack faces. A comparison between results from numerical analyses with and without contact has been performed for the three crack depths $a/R = 0.2, 0.5$ and 0.8 .

Results extracted along the circumferential coordinate θ , see Figure 11, show that the influence from contact between crack surfaces increases with increasing crack depth, see Figure 12 to Figure 14.

Conservatism is introduced and geometry factors are overestimated when contact between the crack faces is omitted during the simulation. The profile of the geometry factor is symmetric along the circumference when contact is omitted, in contrast to the non-symmetry obtained when contact is included in the simulation.

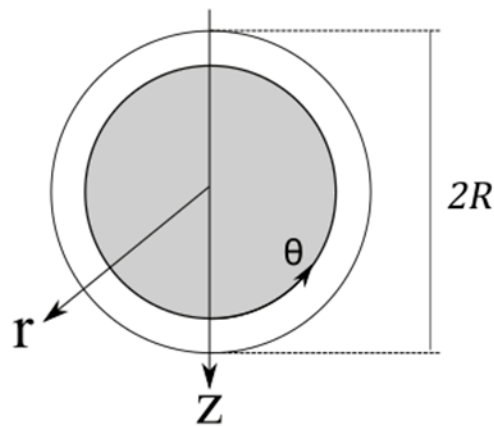


Figure 11 *The influence from contact between crack surfaces was investigated as function of the circumferential coordinate θ .*

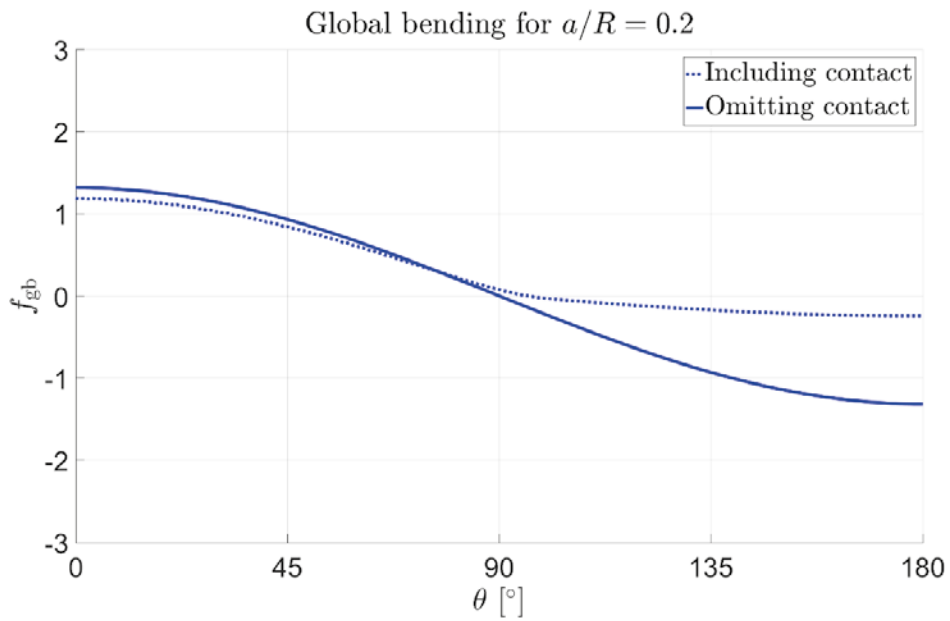


Figure 12 Global bending for the crack depth $a/R = 0.2$ with and without contact applied between the crack faces.

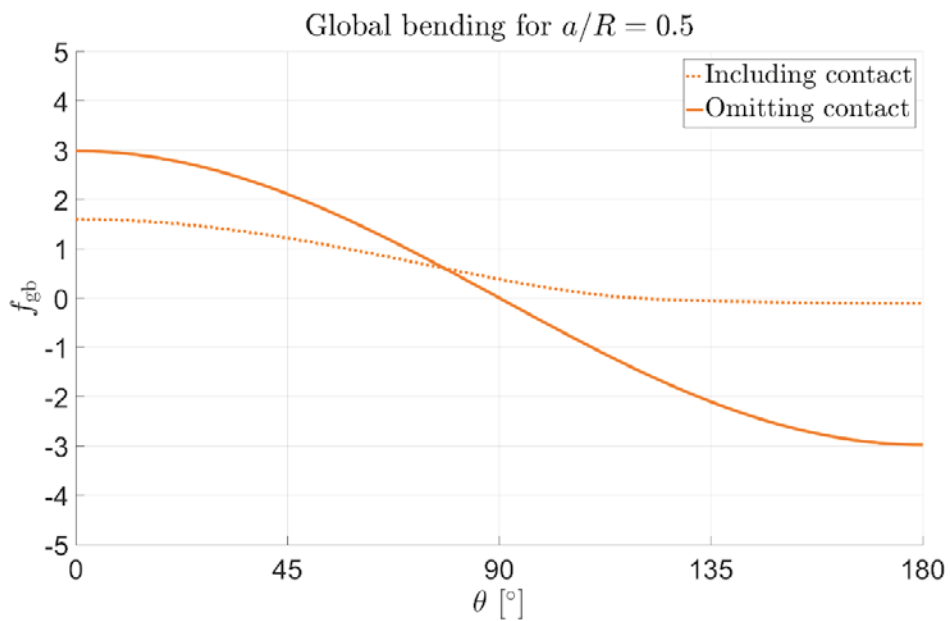


Figure 13 Global bending for the crack depth $a/R = 0.5$ with and without contact applied between the crack faces.

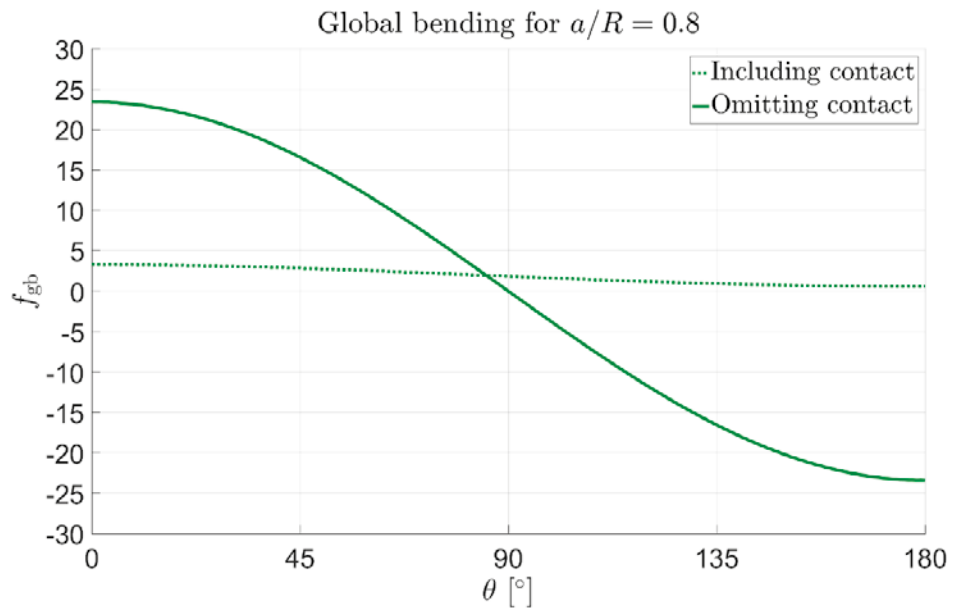


Figure 14 Global bending for the crack depth $a/R = 0.8$ with and without contact applied between the crack faces.



2017:16

The Swedish Radiation Safety Authority has a comprehensive responsibility to ensure that society is safe from the effects of radiation. The Authority works to achieve radiation safety in a number of areas: nuclear power, medical care as well as commercial products and services. The Authority also works to achieve protection from natural radiation and to increase the level of radiation safety internationally.

The Swedish Radiation Safety Authority works proactively and preventively to protect people and the environment from the harmful effects of radiation, now and in the future. The Authority issues regulations and supervises compliance, while also supporting research, providing training and information, and issuing advice. Often, activities involving radiation require licences issued by the Authority. The Swedish Radiation Safety Authority maintains emergency preparedness around the clock with the aim of limiting the aftermath of radiation accidents and the unintentional spreading of radioactive substances. The Authority participates in international co-operation in order to promote radiation safety and finances projects aiming to raise the level of radiation safety in certain Eastern European countries.

The Authority reports to the Ministry of the Environment and has around 300 employees with competencies in the fields of engineering, natural and behavioural sciences, law, economics and communications. We have received quality, environmental and working environment certification.

Strålsäkerhetsmyndigheten
Swedish Radiation Safety Authority

SE-171 16 Stockholm
Solna strandväg 96

Tel: +46 8 799 40 00
Fax: +46 8 799 40 10

E-mail: registrator@ssm.se
Web: stralsakerhetsmyndigheten.se